# Low RCS and Broadband ME Dipole Antenna Loading Artificial Magnetic Conductor Structures

*Chen ZHANG, Xiang-yu CAO, Jun GAO, Si-jia LI, Yue-jun ZHENG*

Information and Navigation Institute of Air Force Engineering University, Xi'an, Shaanxi, 710077, China

xue320long@sina.cn, xiangyucaokdy@163.com, gjgj9694@163.com, lsj051@126.com, erikzhengyang@126.com

Submitted July 22, 2016 / Accepted September 24, 2016

**Abstract.** *A design for low radar cross section (RCS) and broadband magnetic-electric (ME) dipole antenna is proposed. Minkowski-like fractal metal patches printed on the substrate form the electric dipoles, four metallic vias connected to the radiation patches and the metal ground form the magnetic dipoles. The whole antenna is connected with an L-shaped feeding structure which excites electric and magnetic dipoles simultaneously. Meanwhile, two different structure AMC cells with a 180° (±30°) phase difference in a broadband frequency region are designed as a chessboard and loaded around the ME antenna radiation patch. Numerical and experimental results incident the antenna bandwidth is 42.4 % from 8.0 GHz to 12.3 GHz, covering the whole X band. Moreover, the RCS is reduced remarkable in a broad frequency range from 6.5 GHz to 15.5 GHz (81.8 % relative bandwidth) when compared to conventional ME antenna. After loading AMC structures, the antenna still keeps advanced performances such as stable gain and almost consistent pattern in E and H plane.*

## Keywords

Broadband, RCS reduction, ME dipole antenna, AMC

## 1. Introduction

Microstrip antennas have been widely used in the battlefield communication, surveillance and weapon platform owing to its small size, low profile-configuration and easy integration characteristics. However, the narrow impedance bandwidth problem makes them unable to be applied in the wideband antenna system, meanwhile, the radiation pattern changes substantially in E and H plane across the bandwidth [1]. These disadvantages restrict the application ranges of the microstrip antennas.

In the recent few years, a novel type of complementary antenna named magneto-electric (ME) dipole antenna has a significant development [2–4]. The elementary ME antenna is a type of wideband and unidirectional radiation antenna. Owing to its excellent electrical characteristics such as low cross polarization, low back-lobe radiation, stable gain across the operating band, as well as nearly identical E and H plane unidirectional radiation patterns [2–5], it can potentially satisfy the needs of modern wireless communication system. In 2006, a novel wideband antenna, designated as ME dipole was firstly invented by Luk and Wong [6]. Later, a series of ME antennas was developed for different frequencies and applications [7, 8]. However, ME antennas have not been applied in the battlefield domains for the great contribution to the overall radar cross section (RCS), it will influence the stealth performance of the platform and the stealth system will be worthless [9]. Many methods have been presented to reduce the RCS of the antennas, such as miniaturizing the antenna size and adopting radar absorbing material [10]. The above two methods, especially the conventional radar absorbing technique, have negative influence on the radiation performance of the antennas and the RCS reduction bandwidth is narrow. Consequently, it is a challenge to reduce the antenna RCS in wideband and without degrading the radiation performance [11].

In recent years, metamaterial has an important application foreground in antenna RCS reduction [12–14]. [15] designed a novel frequency selective absorbing ground plane, after loading to microstrip antenna arrays, a wideband RCS reduction is achieved over the range of 4 GHz to 12 GHz. [16] presented a slot array using polarization conversion metasurfaces, the relative RCS reduction bandwidth reached to 116 % from 5.85 GHz to 18 GHz, meanwhile, the antenna radiation characteristics were well preserved. Artificial magnetic conductor (AMC) can also be applied to RCS reduction area. In this letter, we proposed a novel ME dipole microwave antenna covering the whole X-band. The antenna has stable gain and nearly identical E and H plane unidirectional radiation patterns. Meanwhile, two different structure AMC cells with a 180° (±30°) phase difference in a broadband frequency region are designed as a chessboard and loaded around the ME antenna radiation patch. Numerical and experimental results incident that, by loading the AMC structures, a broadband RCS reduction including the in-band RCS reduction is achieved compared to the conventional ME antenna, moreover, the ME antenna still keeps advanced performances.

# 2. Analysis and Design of AMC Structures

According to theoretical analysis of phase cancellation two AMC structures are designed in this paper, respectively named AMC1 and AMC2.

## 2.1 RCS Reduction Analysis

Assuming the two structures have the same reflection field when a plane wave illuminates, which are respectively represented by

$$E_{\mathrm{AMC}_1} = A \cdot \exp\left(\mathrm{j} \cdot \varphi_1\right), \tag{1}$$

$$E_{\mathrm{AMC}_2} = A \cdot \exp\left(\mathrm{j} \cdot \varphi_2\right) \tag{2}$$

where $E_{\mathrm{AMC}_1}$ and $E_{\mathrm{AMC}_2}$ are the reflection field of the two structures, $A$ is the reflection magnitude, $\varphi_1$ and $\varphi_2$ are the reflection phase. The equivalent total reflection is

$$E = E_{\mathrm{AMC}_1} \cdot AF_1 + E_{\mathrm{AMC}_2} \cdot AF_2 . \tag{3}$$

$AF_1$ and $AF_2$ are the array factors, their expressions are

$$AF_1 = \exp\left[\mathrm{j}\left(kx + ky\right)d/2\right] + \exp\left[\mathrm{j}\left(-kx - ky\right)d/2\right] \tag{4}$$

$$AF_2 = \exp\left[\mathrm{j}\left(kx - ky\right)d/2\right] + \exp\left[\mathrm{j}\left(-kx + ky\right)d/2\right]. \tag{5}$$

Thereinto, $x = \sin\theta\cos\varphi$, $y = \sin\theta\sin\varphi$, $\theta$ and $\varphi$ are included angles between the incident wave and $X$, $Z$ axis, $k = 2\pi/\lambda$, $d$ is the centers between $\mathrm{AMC}_1$ and $\mathrm{AMC}_2$. When the plane wave is normally impinging, $AF_1 = AF_2 = 2$, then the total reflection is simply given by

$$E = 2A \cdot \left[\exp\left(\mathrm{j} \cdot \varphi_1\right) + \exp\left(\mathrm{j} \cdot \varphi_2\right)\right] . \tag{6}$$

To have a 10-dB reduction of boresight reflection compared to the PEC surface, the effective phase difference range for cancellation is calculated by the expression

$$\left|E\right|^2 / \left|E_0\right|^2 \le -10\ \mathrm{dB} . \tag{7}$$

$E_0$ is the reflection field of the PEC surface under the same incident wave. That is to say, the effective reflection phase difference between $\varphi_1$ and $\varphi_2$ can be expressed as

$$143^\circ \le \left|\varphi_1 - \varphi_2\right| \le 217^\circ . \tag{8}$$

For simplicity, we consider 180°(±30°) as an effective phase difference. Therefore, if the two AMC structure cells constitute as a chessboard configuration and load around the antenna radiation patch, the RCS should be greatly reduced in this frequency range.

## 2.2 AMC Structure Design

Through the above analysis, two AMC structures are specifically designed as follows, shown in Fig. 1.

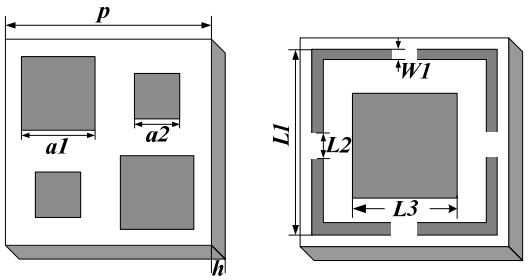


**Fig. 1.** Structures of the two AMC cells.

The two AMC cells are both three-layer structures. Four metal square patches constitute AMC1 cell, square ring with gaps and patch constitute AMC2 cell, both are printed on dielectric slab with a thickness of $h$ = 4 mm. The underside of the substrate is copper without pattern, so that the transmitted wave could be suppressed. Optimization process results in the dimensions depicted in Fig. 1: $p$ = 9 mm, $a1$ = 3 mm, $a2$ = 2.2 mm, $L1$ = 7.2 mm, $L2$ = 1.8 mm, $L3$ = 3.5 mm, $W1$ = 0.4 mm.

Two AMC structures are analyzed at various angles of incidence by Ansoft HFSS using master and slave boundary conditions. The phase reflection characteristics are shown in Fig. 2(a). When the incidence angle is 0°, which means the incident wave is perpendicular to the surface of the AMC cell, the 0° reflection phase point of AMC2 appears at 10 GHz and the phase declines when frequency increases. AMC1 exhibits a 0° phase reflection phase value at two different frequencies: 6.1 GHz and 16.1 GHz and the reflection phase inverses at 10 GH. The phase difference in the range 180°±(30°) is from 6.6 GHz to 15.3 GHz, shown in Fig. 2(b). With the increase of the incidence angle, the reflection phase curves of both two AMC cells shift to higher frequency. When the angle changes from 20° to 40°, the curve of AMC1 shifts obviously, by comparison, the curve of AMC1 generally maintains the same, which means the angular stability of AMC1 is better. Fig. 2(b) also proves the above viewpoint, it can be seen when the incident wave changes to 40°, the effective phase difference has an obvious deterioration. Therefore, only when the angle of incident wave is less than 20°, the two different AMC structures exhibit obvious reflection phase differences across a broad frequency range.

The relevant parameters of the two AMC structures are studied to get the better results. For AMC1, the side lengths of two square patches $a1$, $a2$ are investigated respectively. When one parameter changes, the other remains unchanged, as shown in Fig. 3(a) and Fig. 3(b). It can be seen with $a1$ increasing, the reflection phase shifts to lower frequency. Parameter $a2$ behaves the same law. For AMC2, the slot width $w1$ and the side width of square patch $L1$ are discussed, shown in Fig. 4(a) and Fig. 4(b). Parameter $w1$ has little effect to the reflection phase, the curve remains substantially unchanged. By comparison, $L1$ has obvious impact to AMC2, when $L1$ increases, the reflection phase shifts to lower frequency. By optimizing the parameters, we can obtain the corresponding AMC structures.

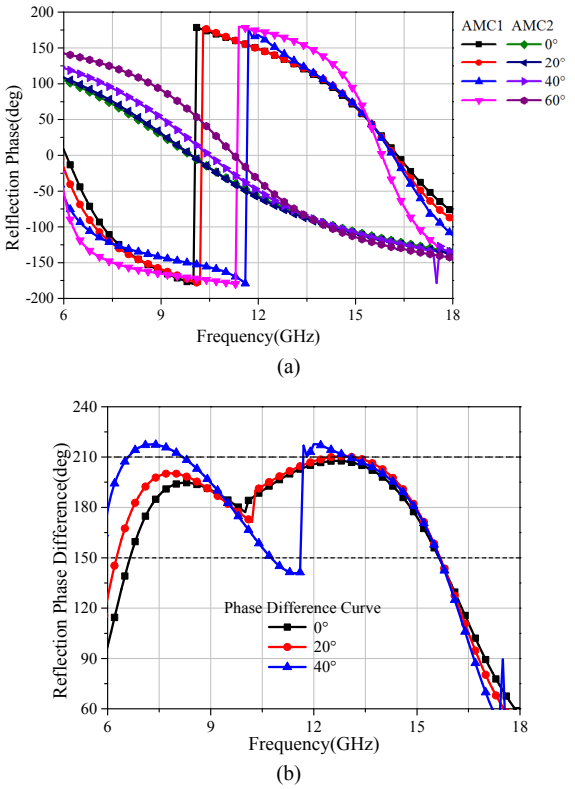


**Fig. 2.** Simulated reflection phase of the AMC cells at various angles of incidence. (a) Reflection phase versus frequency. (b) Phase difference versus frequency

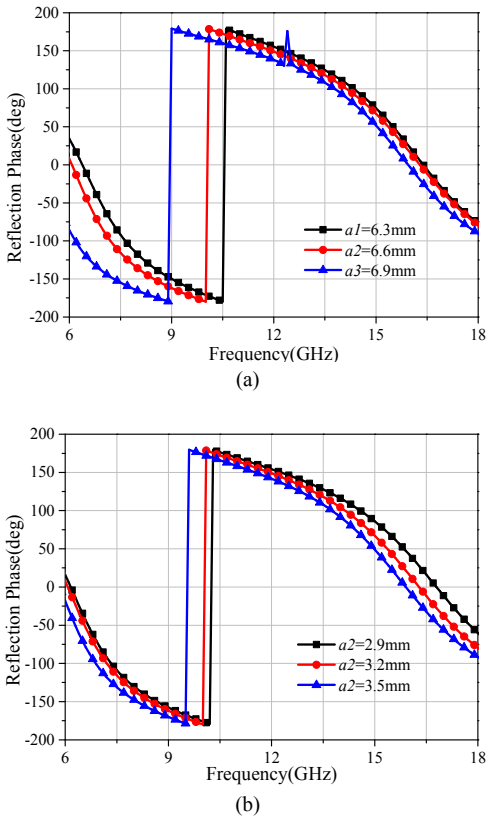


**Fig. 3.** Effects of various AMC1 parameters on the reflection phase performance: (a) side length $a1$, (b) side length $a2$.

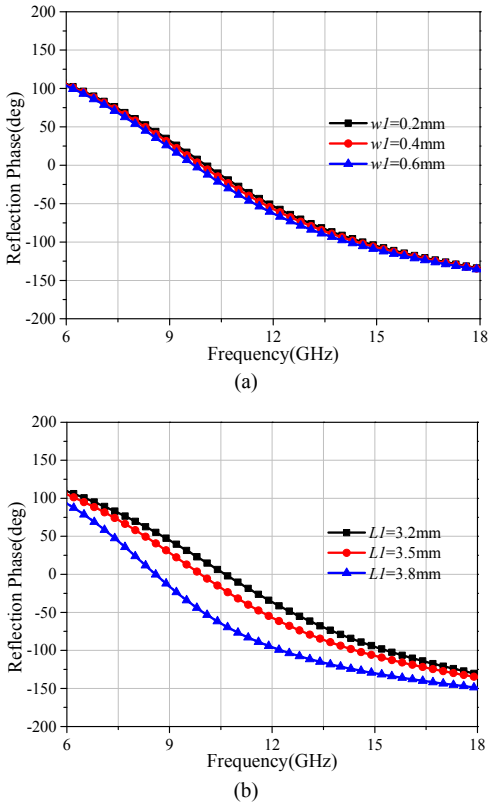


**Fig. 4.** Effects of various AMC2 parameters on the reflection phase performance: (a) slot width $w1$, (b) side width $L1$.

## 3. Design and Analysis of Proposed ME Dipole Antenna

In order to realize the low RCS ME antenna, firstly, the electric dipoles and the magnetic dipoles should be excited simultaneously. Secondly, to attain the nearly identical E and H plane unidirectional radiation patterns, the phase difference between the electric dipoles and the magnetic dipoles has to be adjusted properly. Finally, the RCS reduction problem should be considered. The whole antenna uses the same dielectric slab as the AMC structures, and the radiation part is on the central position. Four Minkowski-like fractal metallic patches form the electric dipole part, metallic vias connected with the ground form the magnetic dipole part. The L-shaped feeding line improves the antenna's matching performance, simultaneously exciting the electric and magnetic dipole. Around the radiation part, two AMC cells constitute block arrays and load. Each AMC block is formed by 3 × 3 AMC1 or AMC2 cells. The chessboard configuration consists of 3 × 3 AMCs block arrays except the middle part. The two AMC structures are analyzed by Ansoft HFSS using master and slave boundary conditions. Master and slave boundaries enable to create models of periodicity. Usually, they are useful for simulating infinite arrays, single AMC unit does not have the corresponding reflection characteristic in application. Therefore, if each AMC block is formed by only 1 AMC cell or 2 × 2 AMC cells, the antenna will not have low RCS char-

acteristic. According to experience, at least 3 × 3 units combined together will behave the ideal characteristic. Using 4 × 4 AMC block or more can also achieve RCS reduction effect compared to the same size antenna, but the size of the antenna itself will increase, therefore, we choose 3 × 3 as the AMC block size. The optimization process results in the dimensions depicted in Fig. 3: $L = 81$ mm, $m = 2.7$ mm, $c = 6$ mm, $s = 5.2$ mm, $v = 1.3$ mm, $w = 1.5$ mm, $q = 1.3$ mm. In order to analyze the properties of the proposed antenna, a reference ME antenna without loading AMC structures is compared, simulated radiation property results are depicted in Fig. 5.

Figure 6(a) shows the reflection coefficients of the proposed and reference antennas, both are coinciding well with each other. The impedance bandwidth of the reference antenna is from 8.1 GHz to 12.7 GHz, after loading AMC structures, the resonant frequencies move toward the lower band, from 8.0 GHz to 12.3 GHz, covering the whole X band.

Figures 6(b) and (c) show the radiation patterns of both the proposed and reference antennas at 9 GHz and 11 GHz, when working at the two different frequencies, the maximum gains both maintain at 8 dBi around, meanwhile, the two antennas both have nearly identical E and H plane unidirectional radiation patterns. Figure 6(d) explains the working principle of the ME antenna, the current distributions at different phases at 10 GHz is simulated. When the phase of exciting signal changes from 0° to 270° at the alternation of the quarter period, the current distributions on the radiation patches, metallic vias and the groundplane vary periodically. At time $t = 0$ and $T/2$, the current mainly distributes on the patches, but the direction is opposite. This means the electric dipoles are strongly excited. However, at time $t = T/4$ and $3T/4$, the currents on the vertically

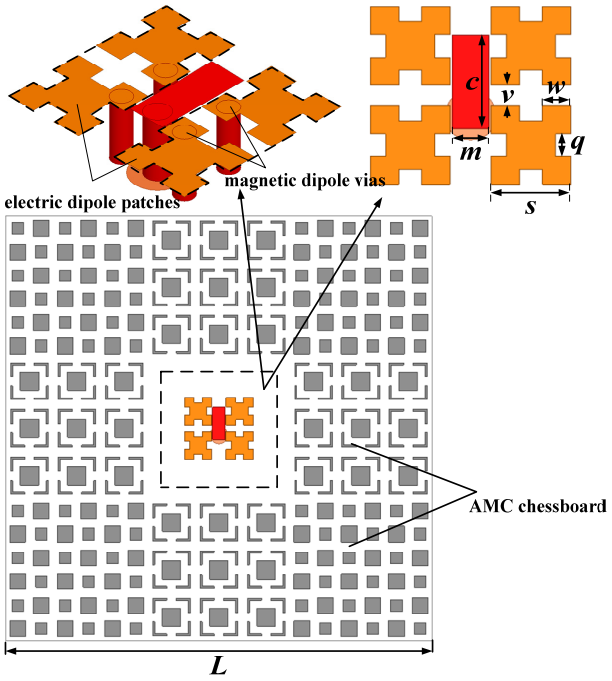


**Fig. 5** Geometry of the proposed antenna.

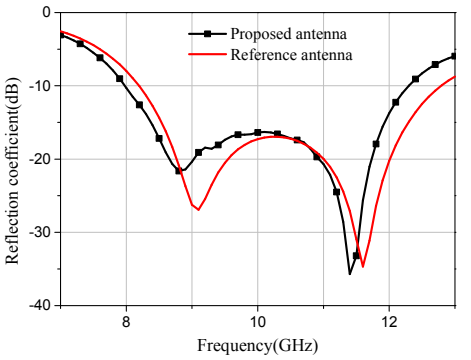


(a)

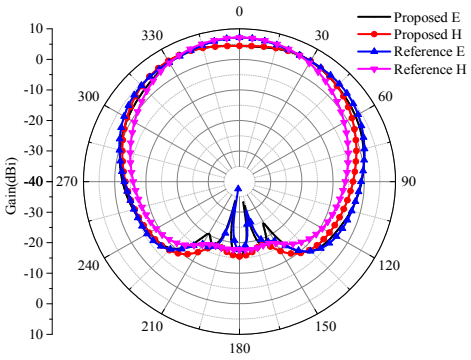


(b)

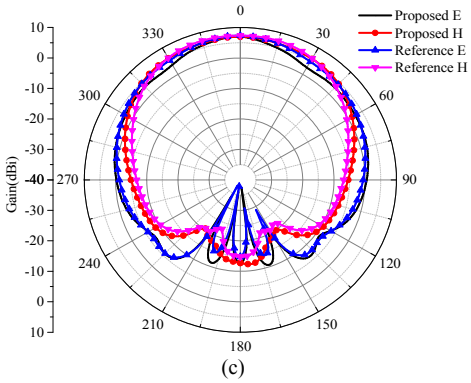


(c)

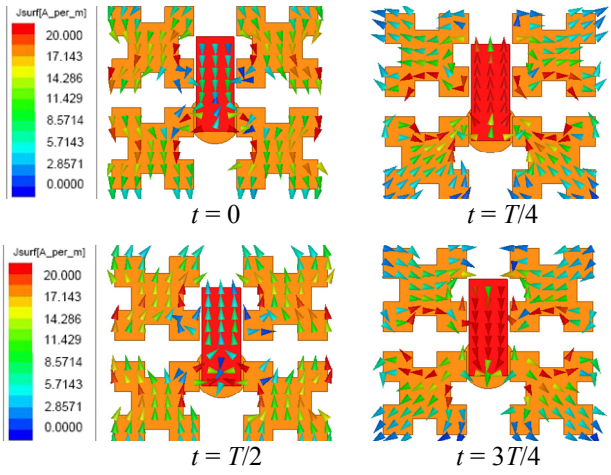


(d)

**Fig.6.** Comparison of simulated reflection coefficients, radiation patterns at 9 GHz, 11 GHz and vector current distributions: (a) reflection coefficients, (b) 9 GHz radiation patterns, (c) 11 GHz radiation patterns, (d) vector current distributions at different times.

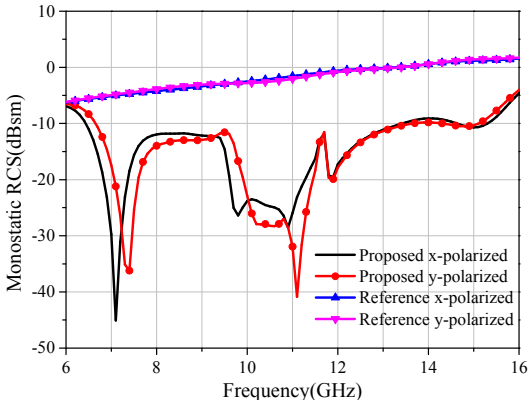


**Fig. 7.** Simulated results of monostatic RCS.

shorted patch antenna reach maximum respectively and are in opposite direction. Hence, the equivalent magnetic and electric currents are along the opposite direction in a period, which confirms that the proposed antenna can generate an enhanced complementary radiation pattern. From the simulated results, it can be observed that the ME antenna still keeps favorable radiation properties after loading AMC structures.

To validate the broadband low RCS characteristic, the monostatic RCS of both the antennas for x-polarized and y-polarized incident waves impinging from normal direction have been simulated, shown in Fig. 7. As predicted, owing to phase cancellation of the two AMC structures, the proposed ME antenna has a broadband RCS reduction compared to the reference one. From 6.5 GHz to 15.5 GHz (81.8 % relative bandwidth), the value of the RCS reduction is always larger than 10 dB for both polarizations. The maximum RCS reduction value reaches 49 dB. For the reduction band covering the antenna working band, both in-band and out-band RCS reduction are achieved. The simulated results certify the accuracy of the antenna design.

## 4. Fabrication and Measurement

To verify the proposed antenna, the prototype design is fabricated and measured. The photograph of the fabricated antenna is shown in Fig. 8. Measured results of reflection coefficient and radiation patterns are attained by Agilent 5230C network analyzer, as shown in Fig. 9. It can be seen the measured $S_{11} < -10$ dB impedance bandwidth is 43.1% ranging from 8.0 to 12.4 GHz, the radiation patterns in E and H plane at 9 GHz and 11 GHz are nearly identical, the gain in the bandwidth is also stable. Figure 9(d) shows

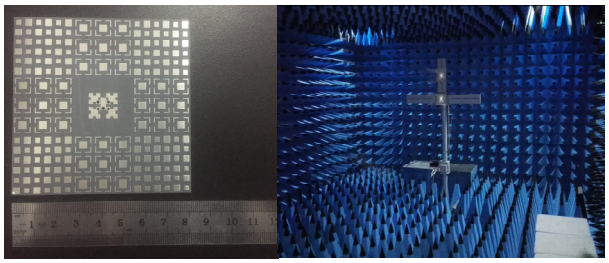

**Fig. 8.** Photograph of the fabricated antenna.

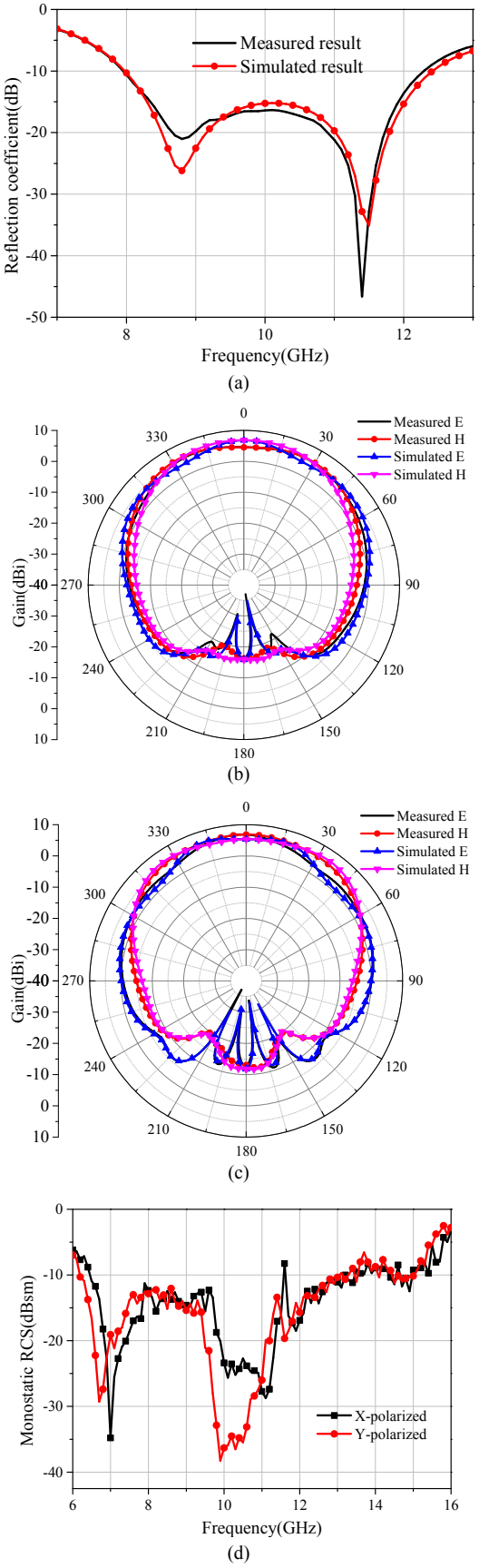


**Fig. 9.** Measured reflection coefficients, radiation patterns and monostatic RCS: (a) reflection coefficients, (b) 9 GHz radiation patterns, (c) 11 GHz radiation patterns, (d) monostatic RCS.

| | [13] | [15] | [16] | This paper |
|---|---|---|---|---|
| Antenna bandwidth (%) | 6 | 1.9 | 7.7 | 42.4 |
| RCS reduction bandwidth (%) | 67 | 100 | 116 | 82 |
| Maximum RCS reduction value (dB) | 17 | 24 | 25 | 49 |

**Tab. 1.** Comparison between the proposed design and existing designs.

the measured RCS result, which is approximately the same as the simulated one. The differences between the simulated and measured results are mainly due to the antenna fabrication errors and the testing environment influences.

In Tab. 1, a comparison between the proposed design and existing designs in both radiation and scattering performance is summarized.

## 5. Conclusion

A low RCS and broadband ME dipole antenna loading AMC structures is proposed in this letter. The bandwidth is 42.4 % from 8.0 GHz to 12.3 GHz, covering the whole X band. Meanwhile, by loading two AMC structures around the patches as a chessboard configuration, both in-band and out-band RCS are reduced. Moreover, the antenna still keeps excellent electrical characteristics such as stable gain, low back-lobe radiation and nearly identical E and H plane unidirectional radiation patterns. It has a broad application prospect in antenna stealth system.

## Acknowledgments

This work is supported by the National Natural Science Foundation of China under Grant (No.61271100, No.61471389, No. 61501494, and No.61671464). Authors also thank the reviewers for their valuable comments.

## References

[1] BAI, Y., XIAO, S., TANG, M., et al. Wide-angle scanning phased array with pattern reconfigurable elements. *IEEE Transactions on Antennas and Propagation*, 2011, vol. 59, no. 11, p. 4071–4076. DOI: 10.1109/TAP.2011.2164176

[2] FENG, B., AN, W., DENG, L., et al. Dual-wideband complementary antenna with a dual-layer cross-ME-dipole structure for 2G/3G/LTE/WLAN applications. *IEEE Antennas and Wireless Propagation Letters*, 2015, vol. 14, p. 626–629. DOI: 10.1109/LAWP.2014.2375338

[3] LUK, K., WU, B. The magneto-electric dipole, a wideband antenna for base stations in mobile communications. *Proceedings of the IEEE*, 2012, vol. 100, no. 7, p. 2297–2307. DOI: 10.1109/jproc.2012.2187039

[4] GOU, Y., YANG, S., LI, J., NIE, Z. A compact dual-polarized printed dipole antenna with high isolation for wideband base station applications. *IEEE Transactions on Antennas and Propagation*, 2014, vol. 62, no. 8, p. 4392–4395. DOI: 10.1109/TAP.2014.2327653

[5] GE, L., LUK, K. M. Linearly polarized and dual-polarized magneto-electric dipole antennas with reconfigurable beam width in the H-plane. *IEEE Transactions on Antennas and Propagation*, 2016, vol. 64, no. 2, p. 423–431. DOI: 10.1109/TAP.2015.2505000

[6] LUK, K.M., WU, B.Q. A new wideband unidirectional antenna element. *Microwave and Optical Technology Letters*, 2006, vol. 1, no. 1, p. 35–44.

[7] WU, B.Q., LUK, K.M. A wideband dual-polarized magneto-electric dipole antenna with simple feeds. *IEEE Antennas and Wireless Propagation Letters*, 2009, vol. 8, p. 60–63. DOI: 10.1109/LAWP.2008.2011656

[8] YAN, S., SOH, P. J., VANDENBOSCH, G. Wearable dual-band magneto-electric dipole antenna for WBAN/WLAN application. *IEEE Transactions on Antennas and Propagation*, 2015, vol. 60, no. 9, p. 4165–4169. DOI: 10.1109/TAP.2015.2443863

[9] ESMAELI, S. H., SEDIGHY, S. H. Wideband radar cross-section reduction by AMC. *Electronics Letters*, 2016, vol. 52, no. 1, p. 70 to 71. DOI: 10.1049/el.2015.3515

[10] LI, S., GAO, J., CAO, X., et al. Multiband and broadband polarization-insensitive perfect absorber devices based on a tunable and thin double split-ring metamaterial . *Optics Express*, 2015, vol. 23, no. 3, p. 3523–3533. DOI: 10.1364/OE.23.003523

[11] LIU, Y., WANG, H., LI, K., GONG, S. RCS reduction of a patch array antenna based on microstrip resonators. *IEEE Antennas and Wireless Propagation Letters*, 2015, vol. 14, p. 4–7. DOI: 10.1109/LAWP.2014.2354341

[12] LI, S., GAO, J., CAO, X., et al. Wideband, thin, and polarization-insensitive perfect absorber based the double octagonal rings metamaterials and lumped resistances. *Journal of Applied Physics*, 2014, vol. 116, p. 043710. DOI: 10.1063/1.4891716

[13] LI, S., CAO, X., XU, L., et al. Ultra-broadband reflective metamaterial with RCS reduction based on polarization convertor, information entropy theory and genetic optimization algorithm. *Scientific Reports*, 2016, vol. 6, p. 37409. DOI: 10.1038/srep37409

[14] EDALATI, A., SARABANDI, K. Wideband, wide angle, polarization independent RCS reduction using nonabsorptive miniaturized-element frequency selective surfaces. *IEEE Transactions on Antennas and Propagation*, 2014, vol. 62, no. 2, p. 747–753. DOI: 10.1109/TAP.2013.2291236

[15] COSTA, F., GENOVESI, S., MONORCHIO, A. A frequency selective absorbing ground plane for low-RCS microstrip antenna arrays. *Progress in Electromagnetics Research*, 2012, vol. 126, p. 317–332. DOI: 10.2528/PIER12012904

[16] LIU, Y., LI, K., JIA, Y., et al. Wideband RCS reduction of a slot array antenna using polarization conversion metasurfaces. *IEEE Transactions on Antennas and Propagation*, 2016, vol. 64, no. 1, p. 326–331. DOI: 10.1109/TAP.2015.2497352

## About the Authors…

**Chen ZHANG** was born in Shannxi. He received his M.S. degree from the Air Force Engineering University (AFEU) in 2014. He currently works towards his Ph.D. degree. In his research, he specializes in Artificial Magnetic Conductor, antenna design and RCS reduction techniques.

**Xiang-yu CAO** received her M.S. degree from the Air Force Missile Institute in 1989. In the same year, she joined the Air Force Missile Institute. She received her Ph.D. degree in the Missile Institute of AFEU in 1999. From

1999 to 2002, she was engaged in postdoctoral research in Xidian University, China. She was a Senior Research Associate in the Dept. of Electronic Engineering, City University of Hong Kong from June 2002 to Dec. 2003. She is currently a professor and a senior member of IEEE. Her research interests include computational electromagnetic, electromagnetic metamaterials and their antenna applications.

**Jun GAO** received the B.Sc and M.A.Sc degrees from the Air Force Missile Institute in 1984 and 1987, respectively. He joined the Air Force Missile Institute in 1987 as an assistant teacher. He became an associate professor in 2000. He is currently a professor of the Information and Navigation College, Air Force Engineering University of CPLA. He has authored and coauthored more than 100 technical journal articles and conference papers, and holds one China soft patent. His research interests include smart antennas, electromagnetic metamaterials and their antenna applications.

**Si-jia LI** received his M.S. and Ph.D. degrees from the Information and Navigation Institute, AFEU, in 2012 and 2016, respectively. He is currently engaged in postdoctoral research with the same University. His research interests are electromagnetic metamaterials and their antenna applications.

**Yue-jun ZHENG** received his M.S. degree from AFEU in 2013. He is currently working toward the Ph.D. degree. His research interests include microstrip antenna and electromagnetic scattering theory.